

World Water Resources

Bonifacio Fernández
Jorge Gironás *Editors*

Water Resources of Chile

 Springer

Preface

Water is the most critical resource for the sustainable development and management of a country, its society, economy, territory, and the environment. Understanding and characterizing water resources, their space and temporal dynamics and occurrence, as well as their uses, is thus essential. Several views, approaches, disciplines, tools, and data sources are needed in such task; unfortunately, a single reference integrating all this is rarely available. This void is what motivates this book.

Water Resources in Chile attempts for a complete characterization of the status of the hydrologic research and practice in Chile, as well as the up-to-date situation about water research, uses, threats, and challenges. The book corresponds to a major effort involving leading researchers and practitioners with a large expertise and background in hydrology and water resources in the country. After Chap. 1, which presents a brief country profile, there are 21 more chapters addressing a wide variety of subjects. Chapters 2, 3, 4, 5, 6, 7, 8, 9, and 10 cover different topics related to hydrology and sources of fresh water. Chapters in this section deal with climate and weather, precipitation, hydrometeorological regimes, surface and groundwater resources, snow processes and glaciers, floods and droughts, water quality, and the recently developed general water balance for the country. Chapter 11 introduces the policy framework of water resources and river basin management in Chile, while Chaps. 12, 13, 14, 15, 16, and 17 describe the agricultural, domestic, mining, hydroelectric, forestry, and environmental water uses in the country. Finally, Chap. 18, 19, 20, 21, and 22 address several issues of interest for water management, including economic and legal aspects of water in Chile, the impact of climate change and land-use changes in water resources, an analysis of current research in water-related issues, and a closing chapter dedicated to the challenges with which the country must cope to ensure a sustainable water use in the future.

We, the invited Editors as well as all the authors, are pleased to contribute with this book to the Springer series “World Water Resources”. We believe the Chilean case will be of interest for the international community, due to the wild disparities in the country’s geography and climate, the frequent occurrence of water-related extreme events, the highly relevant role of snowmelt and groundwater, the variety of

water uses and stakeholders, the particular social and legal framework, and the overall status of a country aiming to become a developed nation, with many fundamental social issues yet to be resolved.

Santiago, Chile

Bonifacio Fernández and Jorge Gironás

Contents

1	Country Profile	1
	Jorge Gironás, Bonifacio Fernández, and José Saldías	
2	Climate and Weather in Chile	7
	Patricio Aceituno, Juan Pablo Boisier, René Garreaud, Roberto Rondanelli, and José A. Rutllant	
3	Precipitation, Temperature and Evaporation.	31
	Lina Castro and Jorge Gironás	
4	Surface Water Resources	61
	Eduardo C. Varas and Eduardo V. Varas	
5	Groundwater Resources.	93
	Francisco Suárez, Sarah Leray, and Pedro Sanzana	
6	Snow Cover and Glaciers	129
	James McPhee, Shelley MacDonell, and Gino Casassa	
7	Floods	153
	Jorge Gironás, Tomás Bunster, Cristián Chadwick, and Bonifacio Fernández	
8	Droughts.	173
	Bonifacio Fernández and Jorge Gironás	
9	Catchment-Scale Natural Water Balance in Chile.	189
	Nicolás Vásquez, Javier Cepeda, Tomás Gómez, Pablo A. Mendoza, Miguel Lagos, Juan Pablo Boisier, Camila Álvarez-Garretón, and Ximena Vargas	
10	Water Quality	209
	Pablo Pastén, Alejandra Vega, Katherine Lizama, Paula Guerra, and Jaime Pizarro	

11 River Basin Policy and Management	229
Humberto Peña	
12 Agricultural Uses	243
Francisco Meza, Pilar Gil, and Oscar Melo	
13 Domestic Uses of Water	259
María Molinos-Senante and Guillermo Donoso	
14 Mining and Industrial Uses	273
Denisse Duhalde, Daniela Castillo, Ricardo Oyarzún, Jorge Oyarzún, and José Luis Arumí	
15 Hydroelectric Uses	285
Sebastián Vicuña, Marcelo Olivares, Chris Hermansen, Mark Falvey, and Fernando Purcell	
16 The Chilean Forest Sector and its Relationship with Water Resources	301
Roberto Pizarro-Tapia, Alfredo Ibáñez-Córdova, Pablo García-Chevesich, Carlos Vallejos-Carrera, Claudia Sangüesa-Pool, and Romina Mendoza-Mendoza	
17 Environmental and Recreational Uses	317
Francisco Riestra, Agustín Silva, and Christian Valenzuela	
18 Economics of Water Resources	335
Guillermo Donoso	
19 Impacts of Climate Change on Water Resources in Chile	347
Sebastián Vicuña, Ximena Vargas, Juan Pablo Boisier, Pablo A. Mendoza, Tomás Gómez, Nicolás Vásquez, and Javier Cepeda	
20 Impacts of Urbanization and Land Use Change over Water Resources	365
Tomás Bunster, Jorge Gironás, Carolina Rojas, and Carlos Bonilla	
21 Water Resources Research in Chile	389
José Vargas and Jorge Soto	
22 Challenges for the Future	409
Bonifacio Fernández, Magdalena Barros, and Jorge Gironás	

Chapter 2

Climate and Weather in Chile



Patricio Aceituno, Juan Pablo Boisier, René Garreaud, Roberto Rondanelli, and José A. Rutllant

Abstract Main physical mechanisms controlling weather and climate in the continental domain of Chile are addressed in this chapter, with particular emphasis on those that are more pertinent to the precipitation regime. In particular, most relevant factors that modulate the rainfall variability, from the intraseasonal time-scale to long-term changes, are discussed in relation with the characteristics of the large-scale atmospheric circulation and different modes in the functioning of the ocean-atmosphere system, and the anthropogenic forcing of climate change.

Keywords Climate · Weather · Precipitation · Rainfall variability · Atmospheric circulation · Ocean-atmosphere system · Climate change

2.1 Introduction

Main physical mechanisms controlling weather and climate in the continental portion of Chile are discussed in this chapter, with particular emphasis on those that are more pertinent to the precipitation regime. Following the presentation in Sect. 2.2 of

P. Aceituno (✉)

Departamento de Geofísica, Facultad de Ciencias Físicas y Matemáticas,
Universidad de Chile, Santiago, Chile
e-mail: aceituno@dgf.uchile.cl

J. P. Boisier · R. Garreaud · R. Rondanelli

CR-2, Centro de Ciencia del Clima y la Resiliencia, Santiago, Chile

Departamento de Geofísica, Facultad de Ciencias Físicas y Matemáticas,
Universidad de Chile, Santiago, Chile

J. A. Rutllant

Departamento de Geofísica, Facultad de Ciencias Físicas y Matemáticas,
Universidad de Chile, Santiago, Chile

CEAZA, Centro de Estudios Avanzados en Zonas Áridas, La Serena, Chile

the large-scale factors influencing climate in this part of the world, including the Pacific Ocean and topography, the characteristics of precipitation episodes and associated mechanisms are addressed in Sect. 2.3. A description of rainfall variability from intraseasonal to interdecadal time scales is presented in Sect. 2.4, while a discussion about the role of coastal low-level stratus clouds along the arid and semi-arid coast of northern Chile as an alternative source of water resource is included in Sect. 2.5.

2.2 Large Scale Factors Controlling Weather and Climate in Chile

The semi-permanent subtropical anticyclone over the Southeast Pacific (SEP) and the westerly wind regime at mid-latitudes are the most relevant large scale atmospheric factors controlling weather and climate in the continental territory of Chile (Fig. 2.1), spanning from around 19°S to 56°S along the western margin of South America (Fuenzalida 1971).

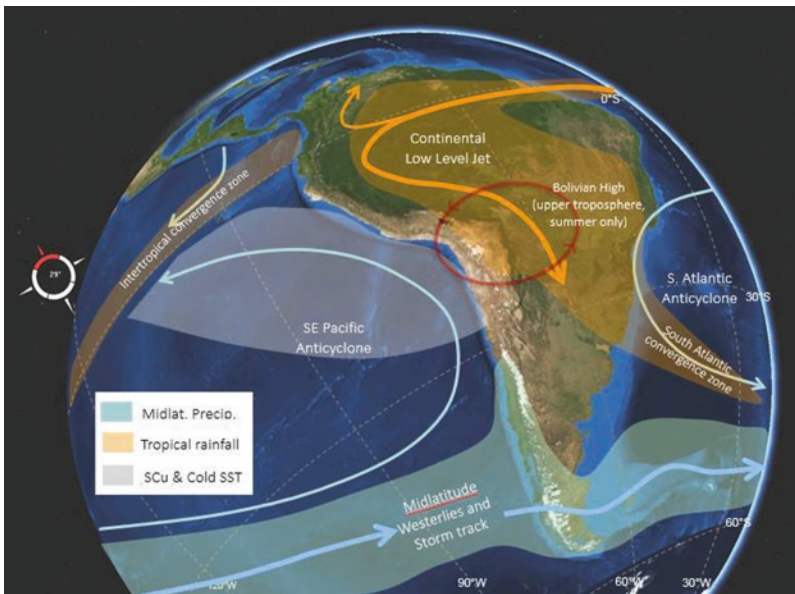


Fig. 2.1 Large scale circulation patterns affecting the hydroclimate of Chile. The cyan and orange curves indicate the circulation near the surface. The red curve indicates the circulation induced by the Bolivian high in the upper troposphere (10 km above sea level, ASL), only evident in austral summer. Cyan and orange shades indicate rainfall produced by extratropical and tropical systems, respectively. Note the effect of the Andes cordillera in extending northward the effect of extratropical storms. The gray shade indicates the typical location of the stratocumulus (low cloud) deck over the SE Pacific

Frontal systems rooted in cyclonic disturbances drifting in the mid-latitude westerly wind belt account for most of the precipitation in south-central Chile, but are restricted by the SEP anticyclone (see Sect. 2.3.2 of this chapter) thus creating a marked north-south precipitation gradient, with annual mean values ranging from less than 10 mm in the hyper-arid north to about 100–1000 mm in the central part, and to more than 3000 mm in the humid southern part of the country (Fig. 2.2a). The southward (northward) displacement of the subtropical anticyclone/westerly wind belt is ultimately forced by the annual cycle of radiative forcing that also controls the annual cycle of air temperature with relative warm (cold) conditions during austral summer (winter) and a marked seasonality in the rainfall regime over the central portion of the country (30°S–40°S) where precipitation episodes concentrate during winter (June–July–August, Fig. 2.2b).

The cold Pacific northward Humboldt current exerts a strong homogenizing effect on the temperature regime along the coast, explaining a meridional gradient that is significantly weaker than that observed on the average for same latitudes at the hemispherical scale. Furthermore, the strong temperature inversion layer separating the relatively cold and humid atmospheric boundary layer from the relatively warmer air mass subsiding above, impose an upper limit to the vertical development of the stratus cloud deck stretching over a large oceanic region within the domain of the SEP subtropical anticyclone.

Topography plays a significant role in shaping the characteristics of weather and climate in Chile. Apart from the barrier effect of the Andes, that isolates the Chilean territory from the influence of continental air masses, particularly in the northern and central portion of the country, the topography modulates the regional and local spatial distribution of rainfall. Forced uplift of air masses on the windward side of the mountains enhances rainfall intensity while subsidence on the leeside reduces it.

Although separated by the formidable Andes cordillera, conditions over the interior of the continent also influence the Chilean climate and weather, especially during austral summer (January–February–March) over the Altiplano region in the central Andes (15–22°S) as explained in Sect. 2.3.1. Summer rainfall episodes linked to continental processes can also occur down to 35°S but limited to the upper parts of the Andes cordillera (Viale and Garreaud 2014).

2.3 Precipitation Episodes and Associated Mechanisms

No matter where we look along continental Chile, the yearly rainfall accumulation is the result of well-defined precipitation events lasting a few days. As reviewed in this section, the number, nature and seasonality of these events varies greatly with latitude. Precipitation in the northern highlands (Altiplano region) is mostly caused by convective storms that develop preferentially in the afternoon and evening during austral summer (December–January–February) in connection with the South American Monsoon at tropical latitudes (e.g. Vera et al. 2006). Central and southern Chile are mostly affected by cold fronts rooted in

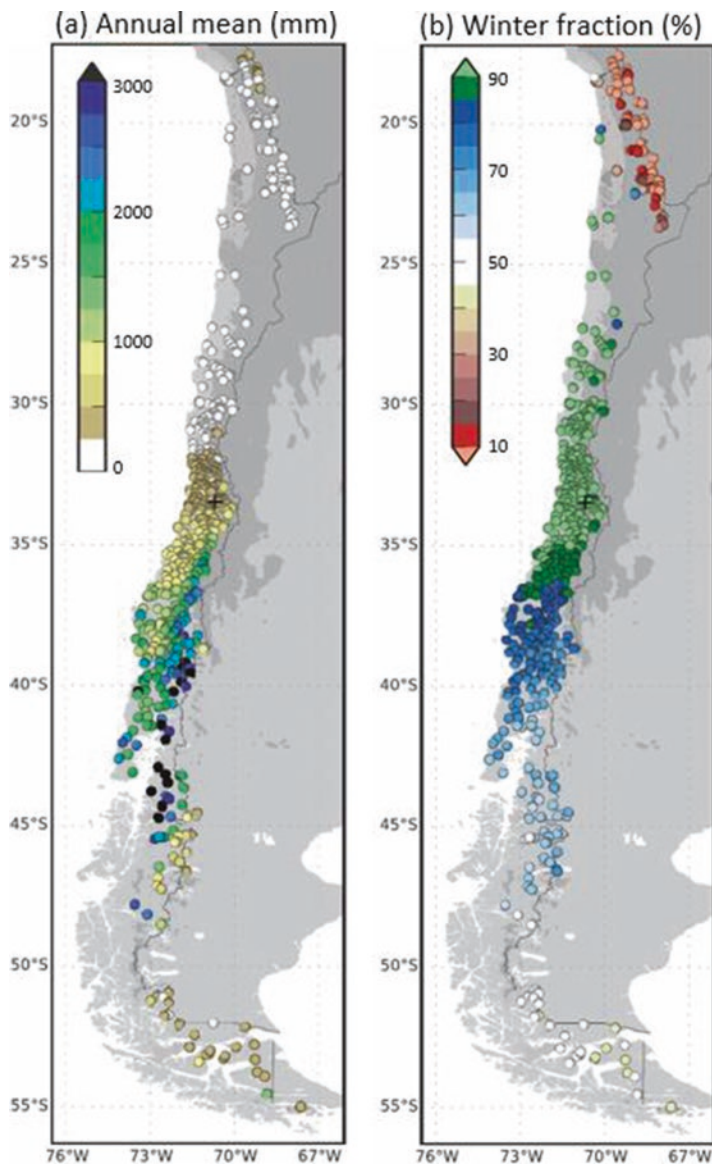


Fig. 2.2 Where and when does it rain along Chile? (a) Mean annual precipitation (mm) in local observational sites. (b) The contribution (%) of rainfall during the austral winter semester (April–September) to annual totals in each site. (Data source: National Weather Service (DMC) and National Water Agency (DGA). Adapted from Boisier et al. 2018)

midlatitude cyclones, more prevalent during winter months, although cut off lows and zonal atmospheric rivers (stationary fronts) can also deliver substantial rainfall throughout the year. The annual fraction of rainy days increases from less than

10% at 30°S to nearly 75% at 45°S (Viale and Garreaud 2015). Farther south the lack of local records along the coast difficult this assessment, but one may speculate an increased fraction of rainy days and a decrease in the seasonality of the rainfall regime.

2.3.1 Rainfall Events in the Altiplano Region

The Altiplano is a high level plateau (ground level at about 3800 m ASL) extending along the central Andes from about 15–23°S, whose climate has been described by Aceituno (1996) and Garreaud et al. (2003), among others. During most of the year, the central Andes are exposed to westerly winds in the middle and upper troposphere that bring dry air, hindering rainfall in the Altiplano. During the austral summer, however, an upper level anticyclone develops over the central part of the continent (the so called Bolivian High), in response to heating over the central part of the continent (Lenters and Cook 1997), leading to weak easterly winds atop of the central Andes. When the easterlies are strong enough, moist air sourced in the Amazon basin and Bolivian lowlands is entrained into the plateau, feeding precipitation events that can last several days interrupted by dry periods of similar duration (Garreaud 1999; Garreaud and Aceituno 2001), as shown in Fig. 2.3a for the location of Chungará. Rainy events are not truly continuous; given their convective nature, intense precipitation (rain, snow and hail), accompanied by lighting, most often occurs during evening but convection subdues during night and is typically absent in the morning hours.

Satellite imagery in Fig. 2.3b illustrates the mesoscale structure of the convective activity, with distinct cores of about 50 km in the horizontal dimension. Convection can be widespread over the Altiplano but it hardly encompasses the western slope of the Andes (near the Chilean border) where very arid conditions prevail. Yet, summer precipitation over the Altiplano is the only source of groundwater and supply for the springs in the upper part of the Atacama Desert (Houston and Hartley 2003). There is also a marked north-south gradient in precipitation over the Altiplano, with highest values around the Titicaca lake (about 700 mm/year) and minimum over the Salar de Uyuni (<100 mm/year).

2.3.2 Extratropical Systems in Central and Southern Chile

To the south of the dry-diagonal that crosses the west coast of South America between 23°S and 27°S, systems of extratropical origin are responsibly for most of the precipitation in central and southern Chile. Here, most of the precipitation is caused by deep stratiform clouds that develop along cold fronts arching equatorward, as the one shown in Fig. 2.4. The fronts are in turn rooted in surface cyclones

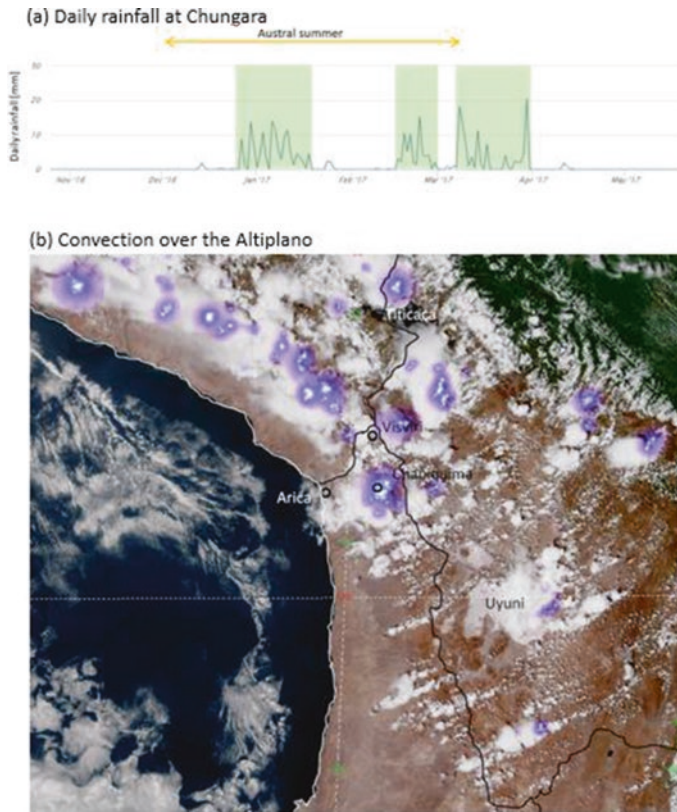


Fig. 2.3 Temporal and spatial characteristics of the summer rainfall over the Altiplano region (northern Chile). (a) Time series of the daily rainfall at Chungará station (18.3°S , 69.1°W , 4570 m ASL) between Dec. 2016 and May 2017. (Data source: National Water Agency (DGA). The green bars encompass 1–2 week long wet periods.) (b) Visible satellite image (from GOES 16) for January 29, 2019 at 17:15 local time. The purple-blue shading represents high density of lightning, indicative of the convective nature of the clouds

drifting eastward in the midlatitudes in connection with upper level troughs. On average the latitudinal position of the storm tracks reaches its northernmost position (45° – 50°S) in austral winter, producing precipitation in central and southern Chile. By the contrary, the storm track moves southward (50° – 55°S) during summer that, together with the expansion of the subtropical anticyclone over the SE Pacific, restrict the precipitation to southern and austral Chile during this season.

Low-level northwesterly flow ahead of a cold front transports warm air with high water vapor content from the subtropical Pacific southward to the west coast of South America. Part of this warm, moist stream ascends over the cold front causing clouds and precipitation over the open ocean but the most significant ascent -and hence precipitation- occurs when the moist-laden air masses approach the impressive Chilean topography. This forced ascent has several consequences. First, it

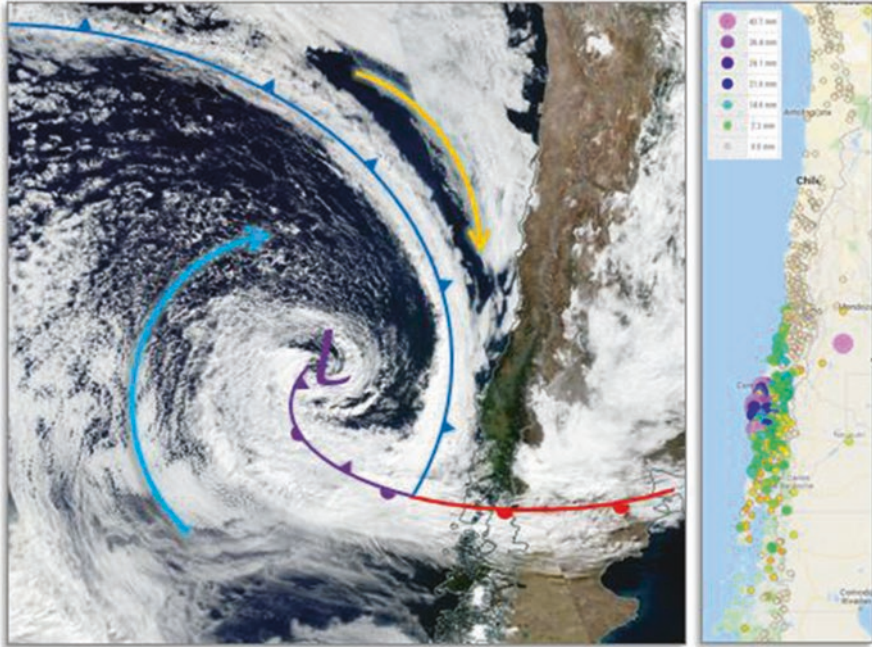


Fig. 2.4 An extratropical storm approaching southern Chile. The left panel is a visible image from the MODIS sensor aboard of the AQUA Satellite for May 5th 2018, at 15:45 UTC. The blue, red and purple lines indicate the location of the cold, warm and occluded fronts, respectively. The light-blue and yellow arrows indicate the low-level flow around the surface depression (low pressure), whose center is identified by the letter L. The right panel shows the station-based total precipitation caused by this system (accumulated rainfall from 4 to 6 of May, 2018). (Data source: National Weather Service (DMC) and National Water Agency (DGA))

produces west-east precipitation gradients at several scales. Between 33°S and 40°S, there is a precipitation maximum along the coast on the windward side of the coastal range and a minimum in the central valley (Falvey and Garreaud 2007; Garreaud et al. 2016). Figure 2.5 illustrates this rainfall contrast for central Chile and the Nahuelbuta mountains in the coast of the Biobío region at about 38°S. To the east of the central valley, precipitation increases by a factor 2–4 over the western slope of the Andes (the Andean amplification is difficult to determine because of the lack of high altitude precipitation records and it also varies significantly among storms), and sharply decreases to the east of the continental divide (Viale and Núñez 2011; Viale and Garreaud 2015). The upstream precipitation enhancement and downstream rain shadow across the southern Andes cordillera creates one of the most extreme precipitation gradients on earth (Smith and Evans 2007), with annual accumulation changing from >3000 to <300 mm within 200 km in the east-west direction across the Patagonia region.

The second consequence of the coastal range and the Andes along central Chile is the blocking of impinging (zonal) flow leading to the formation of a terrain

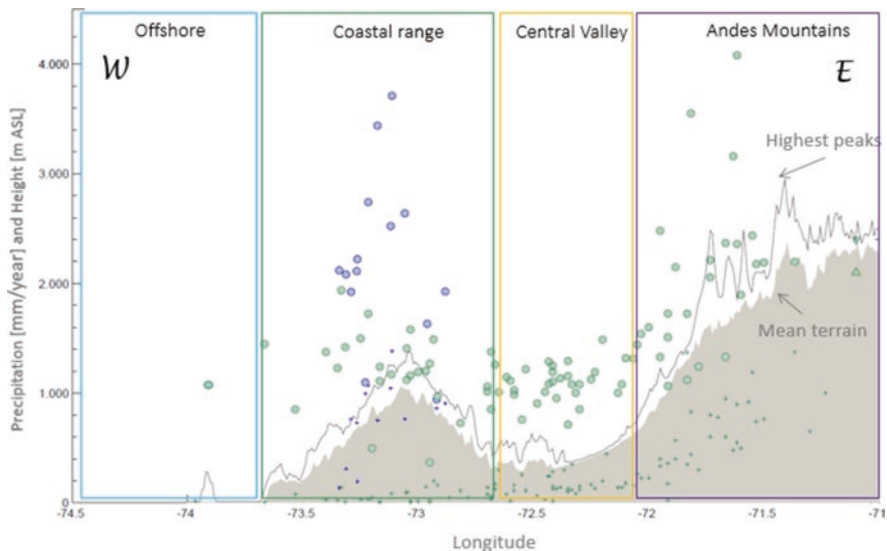


Fig. 2.5 Impact of the topography on precipitation. Circles indicate the mean annual precipitation (MAP) considering all stations between 36.5°S and 38.5°S along a west-east transect (roughly perpendicular to the coastal range and the Andes). Crosses indicate the elevation of these stations (note the absence of high elevation stations in the Andes). The terrain profile is indicated by the mean and maximum height in that range of latitudes. The green circles are MAP from DMC and DGA stations. The blue circles over the coastal range are MAP estimates based on a network of stations installed during AFEX (Garreaud et al. 2017)

parallel, northerly jet (Barrett et al. 2009). During the approach of a cold front, this northerly jet can be very strong, enhancing convergence and rainfall over the Biobío region ($36\text{--}38^{\circ}\text{S}$) but retarding the advance of the front toward central Chile (Barrett et al. 2009). Depending on their speed, air parcels above ~ 2 km can surpass the Andes and deliver precipitation, so that storm-accumulated precipitation at any given latitude is significantly dictated by the strength of the mid-level westerly flow impinging upon the Andes. The correlation between the intensity of this flow and rainfall amount improves slightly if one considers the zonal moisture transport (Falvey and Garreaud 2007) and is also found on longer time scales: the strongest the westerly winds averaged over a season or year, the largest the cumulative precipitation in that period (Garreaud 2007; Garreaud et al. 2013).

In most storms (at least two third of the events) precipitation over the central valley begins almost simultaneously with the arrival of the cold front and the bulk of the rainfall accumulation occurs under cold conditions (post-frontal precipitation), with a freezing level altitude around 2200 m (Garreaud 2013). This level is well below the Andes crest height at subtropical latitudes (>5000 m ASL) so that a substantial portion of the winter precipitation builds up a seasonal snow pack that eventually melts during the next spring-summer season (Cortés et al. 2011). Indeed, many cold fronts arriving to central Chile during winter produce a minor concurrent

increase in the flow of the rivers draining the Andes cordillera. A few winter storms, however, feature warm conditions (air temperature doesn't drop during the precipitation period) causing the freezing level to remain as high as 4000 m ASL, increasing the pluvial area up to a factor 4 relative to average conditions (Garreaud 2013). Warm winter storms have caused some of the most devastating landslides and flooding in the recent past and will be described in connection with zonal atmospheric rivers.

2.3.3 Atmospheric Rivers

The increasing availability of high resolution images of spatial distribution of water vapor and precipitable water (column integrated water vapor content) from meteorological satellites allows the detection of relatively long, narrow regions in the atmosphere, identified as atmospheric rivers (ARs), that transport water vapor outside of the tropics in a concentrated and highly efficient way (for an updated review see Ralph et al. 2017). These features are relevant to the rainfall regime in Chile because those making landfall along the coast favor the occurrence of intense rainfall. Recent surveys of ARs (Guan and Waliser 2015; Viale et al. 2018) indicate that 20–40 ARs make landfall in the coast of central-southern Chile per year (maximum at 40–50°S), one of the largest frequency worldwide, explaining about half of the annual rainfall and extreme precipitation events. Atmospheric rivers are mostly a wintertime phenomenon in central Chile, but they can occur year-round to the south of 40°S.

Most cold fronts described in Sect. 2.3.1 feature an AR ahead of them. ARs can also occur ahead of stationary fronts extending thousands of kilometers across the South Pacific with a zonal (East-West) direction and little displacement in the cross-front (north-south) direction. When a zonal AR landfalls, substantial prefrontal precipitation (up to 100 mm) can accumulate at the coast, inland valleys and the western slope of the Andes over periods of 24–72 h without a decrease in air temperature and freezing levels. As commented before, such situation renders AR/Warm storms into a significant hydrometeorological hazards, such as the 3-May-1993 landslide in Santiago, with a toll of more than 80 fatalities (Garreaud and Rutllant 1996) and the 16-Dec-2017 flooding of the Santa Lucía village in northern Patagonia, with a toll of more than 20 fatalities (Viale 2017). This later case helps to describe the characteristics of a zonal, quasi-stationary AR as depicted in Fig. 2.6. The AR extended more than 3000 km from the central Pacific to South America, and was located just below the axis of the wind maxima that contributed to the exceptional AR length. The upper level flow is mostly zonal, with a hint of a ridge aloft, quite different from the circulation observed most often in winter storms over central Chile (Fig. 2.4) featuring a deep trough aloft and northwesterly flow. Since, in this case there is weak synoptic-scale forcing for upward motion, precipitation (in excess of 80 mm/day) was largely generated by the forced ascent over the Andes of the narrow string of moist air defining the atmospheric river.

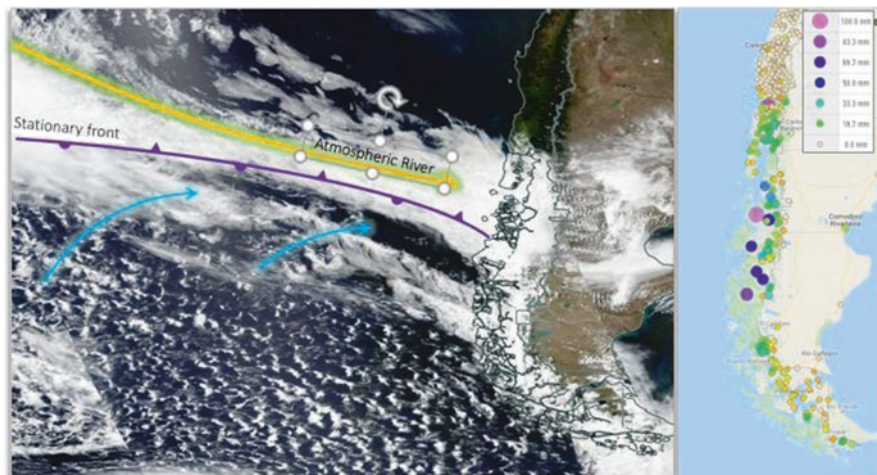


Fig. 2.6 An Atmospheric River (AR) landfalling in southern Chile. The left panel is a visible image from the MODIS sensor aboard of the AQUA Satellite for December 16, 2017, at 15:45 UTC. The purple line indicate the location of a stationary front. The light-blue and yellow arrows indicate the low-level flow at each side of the front. The AR is the stream to the north of the front transporting large amounts of water vapor that cause precipitation when it encounters topography. The right panel shows the station-based total precipitation caused by this AR (accumulated rainfall from 15 to 17 of December, 2017). (Data source: National Weather Service (DMC) and National Water Agency (DGA))

2.3.4 *Cut-Off Lows*

Cut-off lows (COLs) (Palmen 1949) were only recently recognized as potentially relevant for precipitation in Chile, especially in the northern portion of the country (Pizarro and Montecinos 2000; Fuenzalida et al. 2005). Cut-off lows are synoptic scale systems that owe their existence mostly to breaking of the extratropical synoptic scale waves (Ndarana and Waugh 2010). As an upper level trough amplifies towards subtropical latitudes, a cyclonic anomaly becomes disconnected (cut-off) from the high latitude westerly wind regime (see Fig. 2.7). An upper level cyclone is then shed northward reaching even subtropical latitudes along the Chilean coast where it often moves erratically for several days until dissipation or crossing the Andes. The relatively cold mid-tropospheric conditions associated with this system explain the Spanish names given to this phenomenon (“núcleo frío en altura”, upper tropospheric cold core and “gota fría”, cold drop).

A cut-off low is primarily an upper tropospheric phenomenon with circulation and thermodynamic features most evident in the upper levels of the troposphere and surface manifestations hardly present. Nevertheless, COLs are relevant for weather conditions in Chile as they are responsible for a significant fraction of total precipitation in the Northern-Central portion of the country (Barahona 2013). The spatial distribution of precipitation and the fraction of annual rainfall attributed to COLs

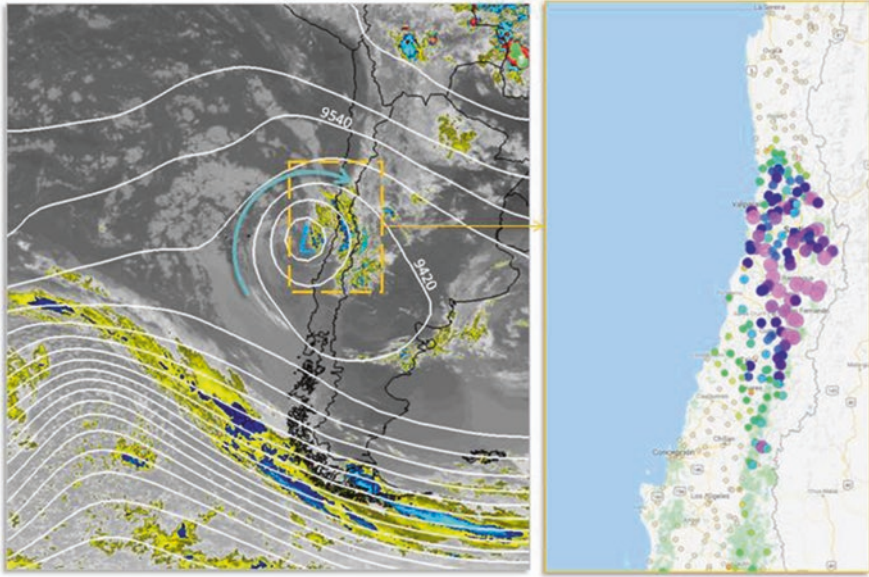


Fig. 2.7 A Cutoff low over central Chile. The left panel is an infrared image from the GOES-12 for March 7, 2008, at about 8 AM. Dark gray areas are cloud free, light gray areas indicate low and midlevel clouds, while yellow and blue areas indicate clouds with high tops, presumably precipitating. Superimpose on this image are the 300 hPa geopotential height contours (every 60 m) showing a cutoff low with its center (L) just offshore central Chile. The right panel shows the station-based total precipitation caused by this COL (accumulated rainfall from 6 to 8 of March 2008). (Data source: National Weather Service (DMC) and National Water Agency (DGA))

are shown in Fig. 2.8 for the period 1979–2014. The contribution of these systems to annual rainfall varies between 0 and 50 mm in the semi-arid region to the north of 32°S while the maximum contribution occurs at about 36°S (with nearly 200 mm/year). Farther north the percentage of annual rainfall associated to COLs can reach 30% or more, although statistics become less reliable with fewer cases detected as one moves into the hyperarid Atacama Desert. In Central Chile, from about 30°S to 38°S, the percentage of annual rainfall due to COLs varies between 10 and 15%.

Besides the impact on annual precipitation, COLs can generate extreme precipitation events, the most recent and noteworthy being the Atacama flooding episode in March 2015 (Barrett et al. 2016; Bozkurt et al. 2016; Rondanelli et al. 2019), one of the worst hydrometeorological disasters in the history of the country in terms of losses of life and infrastructure. Flooding during this storm resulted from the accumulation of up to 100 mm during 3 days over an otherwise arid region, with rainfall intensities in excess of 10 mm/h at some stations.

The relatively cold air associated to COLs induces a decrease in the static stability in mid to lower levels of the troposphere as well as a cyclonic circulation consistent with the field of temperature anomalies. Given that most of these disturbances originate over the cold water of the Southeast Pacific, convective instability is not

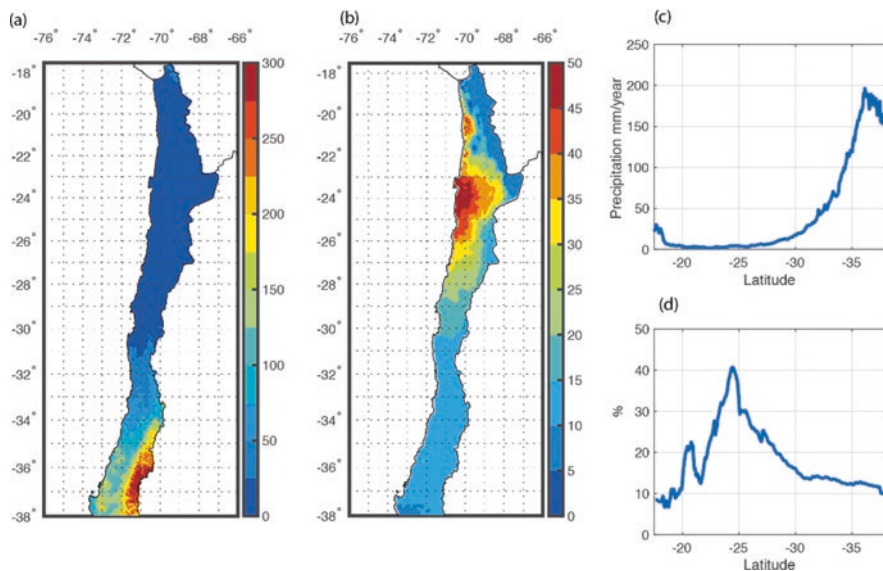


Fig. 2.8 Distribution of annual precipitation due to cut-off lows: (a) spatial distribution and (c) latitudinal distribution from CR2MET daily rainfall product for the period 1979 to 2014 (Boisier et al. 2018), using the cut-off low database developed by Barahona (2016); (b) spatial distribution and (d) latitudinal distribution of the percentage of annual precipitation due to cut-off lows

frequently released over the ocean and consequently dry air masses ascending in the leading edge of the cut-off low explain the relative absence of precipitation over the ocean off the Chilean coast (Garreaud and Fuenzalida 2007; Barahona 2016). Given that a fundamental mechanism for the dissipation of the cut-off low is the heating due to the release of latent heat by water vapor condensation, the cold ocean and the blocking effect of the Andes cordillera act as a “protection” to the release of convective instability and further dissipation of the cut-off low. This might explain the maxima in the frequency of cut-off lows near the Chilean coast (Fuenzalida et al. 2005; Garreaud and Fuenzalida 2007; Barahona 2016).

Different mechanisms control the occurrence of rainfall episodes associated to a cut-off low as it approaches the South American continent, with pre-existing positive sea surface temperature anomalies and larger than average water vapor in the region off the coast of Chile and Peru favoring their occurrence (Fuentes 2014; Bozkurt et al. 2016). In some cases, when water vapor is available from the eastern side of the Andes, deep convection is triggered mostly over the mountains due to the release of conditional instability associated to the forced uplift, usually accompanied by precipitation and thunderstorms. In other cases, when relatively warm conditions prevail, precipitation might concentrate over the coastal region, thereby reversing the typical positive gradient of precipitation with altitude (Scaff et al. 2017).

Cut-off lows are therefore highly relevant for the occurrence of rainfall episodes in Chile, not as much for the total amount of annual precipitation explained by these systems but rather by the potentially large and localized rainfall intensities and

therefore a low spatial predictability of their occurrence, both features arising from the convectively unstable nature of these systems.

2.4 Intraseasonal to Decadal Scale Precipitation Variability

As described in the previous section, the extratropical and oceanic nature of precipitation in most of the Chilean territory is coherent with a marked seasonality and a typical return period (weekly) of rainfall events in winter. Yet, superimposed to the synoptic time scale, there is a myriad of climate variability modes within the Pacific basin that modulates precipitation in Chile within the year (intraseasonal) and in longer time scales (interannual to decadal).

The intraseasonal climate variability in the Southern Hemisphere has been the subject of a large body of research, notably boosted by the increased availability of global weather maps and re-analyses since the 1990s. Beyond the variable observed or method applied, the examination of low-frequency variability of extratropical circulation leads to a coherent picture. The Southern Annular Mode (SAM) and the Pacific–South American (PSA) patterns of variability emerge as the leading intraseasonal modes in this region (e.g., Sinclair et al. 1997; Thompson and Wallace 2000; Mo and Paegle 2001). The SAM (also known as Antarctic Oscillation or high-latitude mode) characterizes a zonally, quasi-symmetric structure in atmospheric fields, measuring the strength of the polar vortex. The PSA patterns refer to stationary wave trains of particularly large amplitude in the south Pacific. The nature of these modes is discussed later.

Figure 2.9 illustrates the influence of intraseasonal circulation variability on precipitation, based on a principal component analysis applied on monthly sea-level pressure (SLP) anomalies in southern extratropical latitudes (20–90°S) for the austral winter semester (April–September). The three leading modes correspond closely to the SAM and PSA modes number 1 and 2 described in former studies (e.g. Sinclair et al. 1997). The first mode measures the co-occurrence of pressure levels below and above normal at mid and high latitudes, respectively, which correspond to the negative SAM phase after a usual definition of this phenomenon (e.g., Marshall 2003). The second mode characterizes high-pressure anomalies around the Amundsen Sea, while the third mode exhibits a wave-like pattern with SLP anomalies of different sign along the Antarctic Circle.

Figure 2.9 also illustrates how the circulation patterns modulate precipitation across the southern Pacific (reanalysis estimate) and in central-southern Chile (observations-based). Within the extratropics, anomalously dry conditions prevail on the equatorward side of the centers of high SLP; a response that can be viewed as the direct – blocking – effect of persistent anticyclones on the westerly flow and baroclinic eddies. In turn, positive precipitation anomalies are found near the centers of negative SLP anomalies. In this way, the first mode (SAM) leads to a band of positive precipitation anomaly at 35–45°S, affecting most of central-southern regions of Chile (Fig. 2.9a; see also Gillett et al. 2006). This effect is consistent with

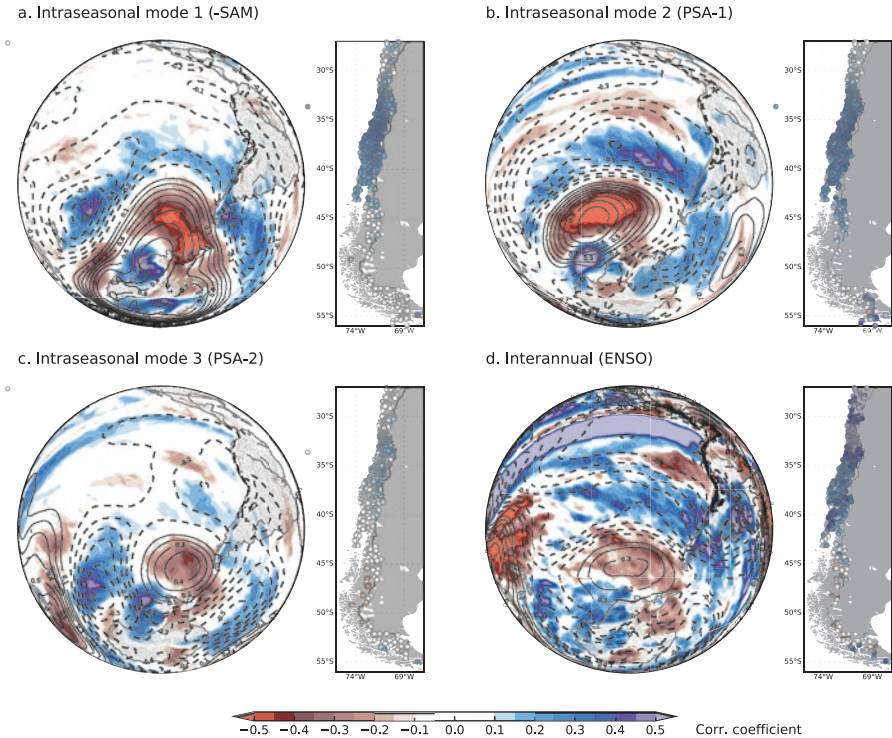


Fig. 2.9 Modes of low frequency variability. (a–c) Pearson's correlation coefficient of the three leading components of monthly sea-level pressure (SLP) anomalies during austral winter (April–September) in the region 20–90°S with SLP (continuous (broken) lines denoting positive (negative) correlation) and precipitation (colored areas). Correlations in panel (d) are obtained between the winter mean multivariate ENSO index (MEI) and SLP/precipitation. Results illustrated in hemispheric maps (left panels) are computed with ERA-Interim reanalysis data (Dee et al. 2011), while details in central and southern Chile (right) are based on observations at stations belonging to the National Weather Service (DMC) and National Water Agency (DGA)

the increased meridional pressure gradient at mid-latitudes and the equatorward location of the storm track during a negative SAM phase (Sinclair et al. 1997; Rao et al. 2003). A similar precipitation pattern is observed in the SE Pacific with the PSA-1 mode, leading to wetter conditions in central and south-central Chile (Fig. 2.9b). In this analysis, the PSA-2 mode comprises an anticyclonic anomaly near the southern tip of South America. Consequently, dry conditions should prevail during the positive phase of this mode in austral Chile, although the limited records in Patagonia do not reflect this effect clearly (Fig. 2.9c). Due to the same mechanism described previously, this mode associates also with positive rainfall anomalies further north in central Chile.

Although the nature of PSA modes is not fully understood (O'Kane et al. 2016), they are frequently linked to standing Rossby waves in the atmosphere, triggered by deep convection in the tropics (Mo and Higgins 1998; Renwick and Revell 1999;

Mo and Paegle 2001). The PSA patterns represent then teleconnections through which a tropical disturbance may affect weather in remote regions. Particularly, this mechanism explains the SE Pacific circulation and South American climate response to some well-known tropical phenomena, notably the Madden-Julian Oscillation (MJO) and El Niño/Southern Oscillation (ENSO) (Aceituno 1988; Karoly 1989; Renwick and Revell 1999; Grimm et al. 2000; Mo and Paegle 2001; Renwick 2005; Barrett et al. 2011; Álvarez et al. 2016).

During the warm ENSO phase (positive MEI Index; El Niño years) there is a tendency for above normal precipitation in central Chile in austral winter and spring. Later in the latter season, these positive rainfall anomalies shift to south-central Chile, while farther south dry anomalies prevail in the austral summer (Rutllant and Fuenzalida 1991; Montecinos and Aceituno 2003). The wetter than normal conditions in central Chile are a regional manifestation of large-scale circulation and precipitation anomalies, as shown in Fig. 2.9d. El Niño leads to anticyclonic circulation anomalies over the Amundsen-Bellinghousen Sea. The stationary and quasi-barotropic nature of these high-pressure systems blocks the westerlies and associated polar-front jet stream, diverting the storm track toward subtropical latitudes (Rutllant and Fuenzalida 1991; Marqués and Rao 1999), where the weakened SE Pacific subtropical anticyclone (SEPSA) favors the development of cyclonic circulation anomalies. The linear, contemporaneous (no lag) relationship between SST anomalies in the tropical Pacific (Niño3.4 index) and central Chile rainfall fluctuated between 0.6 and 0.7 during most of the twenty-first century, enough to consider its use for intraseasonal prediction (Montecinos and Aceituno 2003). During the first decades of the present century, however, the strength of the negative correlation reduced significantly for reasons yet unclear (Garreaud et al. 2019).

ENSO further impacts the rainfall over the South American Altiplano. The weaker than average subtropical jet during La Niña summers (December–January–February) foster advection of moist air from the interior of the continent towards the central Andes (see Sect. 2.3.1) thus increasing rainfall (Garreaud and Aceituno 2001). On the contrary, during El Niño summers stronger than average westerlies in the subtropics restrict rainfall over the Altiplano.

The mechanisms explaining rainfall variability at inter-annual time scales in connection with the ENSO cycle (2 to 7 years) is closely related to intraseasonal phenomena and the occurrence of PSA modes (Fig. 2.9). In particular, when the convective phase of the MJO (30–90 day cycles) transits eastward along the equatorial Pacific from the western side (La Niña-like) to the central Pacific (El Niño-like), a concomitant strengthening and weakening of the SE Pacific subtropical anticyclone is observed. In the later stage, the enhanced convection around the date line triggers a PSA teleconnection (e.g. Álvarez et al. 2016). Therefore, both ENSO and MJO can act constructively to generate circulation anomalies in central Chile that favor the occurrence of intense precipitation episodes (Donald et al. 2006; Juliá et al. 2012; Barrett et al. 2011; Rondanelli et al. 2019).

Given the strong influence of oceanic and atmospheric conditions in the equatorial and South Pacific regions on climate in Chile, its behavior exhibits a decadal-scale variability connected to known ENSO-like, low frequency cycles (e.g.,

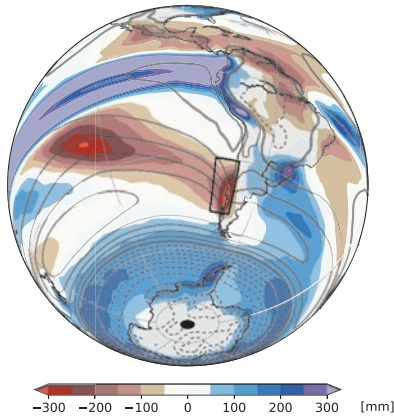
Garreaud and Battisti 1999; Dong and Dai 2015). Following the same mechanisms established for ENSO, warm phases of the Pacific Decadal Oscillation (PDO) or Interdecadal Pacific Oscillation (roughly the same phenomenon) are associated with wetter than normal conditions in central Chile, notably during the 1930s and 1980s. Particular attention has been paid to climate effects of a relatively rapid transition from a negative to a positive PDO phase in the mid-1970s (e.g. Quintana and Aceituno 2012; Jacques-Coper and Garreaud 2015). Moreover, a particularly strong rainfall decline in central Chile since the early 1980s, related to a gradual turn back to a cold PDO phase, has accentuated the effects of a secular drying trend in Chile (Boisier et al. 2016).

2.5 Long-Term Changes in Precipitation

According to what most climate models project for the next decades under carbon-intensive global socioeconomic scenarios, the western coast of southern South America would be one of the regions of the planet strongly affected by precipitation loss (Collins et al. 2013; Schewe et al. 2014; Jiménez-Cisneros et al. 2014). This drying trend, as those modelled in other subtropical regions in the globe (southern Spain and northwestern Africa, south Africa, southwestern Australia), is associated with hemispheric-scale perturbations frequently interpreted as a poleward shift of general circulation patterns, including the expansion of the subtropical dry regimes under influence of descending Hadley Cell branch (Cai et al. 2012). At higher latitudes, an intensification of the circumpolar vortex alike the positive phase of the SAM – shown by both climate models and historical reconstructions (e.g. Gillett et al. 2013) – produces a poleward shift of the region of maximum westerly flow, with dryer/wetter conditions northward/southward from the edge of the mid-latitude storm track. As a result of these large-scale perturbations, current models simulate a particularly strong drying pattern across the SE Pacific, directly heading central-southern Chile (Fig. 2.10), where precipitation may decline by 40% toward the end of the twenty-first century (Polade et al. 2017).

Consistent with the modelled climate response to anthropogenic forcing, observational records indicate a long-term precipitation reduction along the southwest coast of South America (e.g., Aceituno et al. 1993; Minetti et al. 2003; Haylock et al. 2006; Quintana and Aceituno 2012; Cai et al. 2012; Purich et al. 2013), which is particularly significant in central Chile since the end of 1970s. The causes of this trend seem both natural – with the PDO as key driver – and anthropogenic, the latter accounting for about one third of the total signal (Boisier et al. 2016). Further research showed that in addition to the increasing greenhouse gas (GHG) concentration in the atmosphere, changes in atmospheric circulation associated with the stratospheric ozone depletion have very likely contributed to the strong precipitation decline observed in the southern portion of the country during summer (Boisier et al. 2018), a seasonal signature well reproduced in climate model simulations (Fig. 2.10).

a. Projected change in annual Pr. & SLP



b. Projected Pr. in central-southern Chile

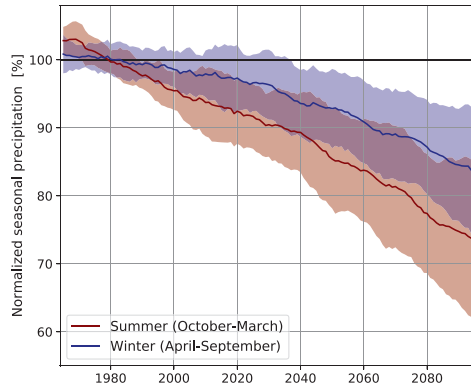


Fig. 2.10 Future climate scenarios: **(a)** Projected multi-model mean change in annual precipitation (colors) and in sea-level pressure (solid and dashed contours indicate positive and negatives differences, drawn every 0.5 hPa) toward the end of the twenty-first century (2060–2099 minus 1960–1999). **(b)** Multi-model mean ± 1 standard deviation of seasonal summer and winter precipitation in central-southern Chile (see domain in panel **(a)**). All results are based on the full-forced historical and rcp8.5 simulations from 34 climate models participating in Coupled Model Intercomparison Project Phase 5 (CMIP5; Taylor et al. 2011)

Since about 2010, the unfortunate combination of a secular drying trend and natural climate variability has resulted in a decade-long rainfall deficit in central Chile. In addition to the multiple impacts driven by reduced water availability, this so-called mega-drought has been accompanied by an above normal frequency of heat waves and more intense fire seasons (Garreaud et al. 2017). The persistence and intensity of this dry period (mean rainfall deficit of $\sim 25\%$) expose a sharp picture of the hydroclimatic conditions that a large region in Chile could face as the norm around the mid-twenty-first century if no strong mitigation measures against fossil-fuel emissions are adopted globally (Fig. 2.10).

Further details on climate scenarios and regional-scale hydrological projections for Chile are included in Chap. 19. Nevertheless, a source of considerable uncertainty in future climate scenarios is the unknown functioning of ENSO in a warmer world, given the high relevance of this mode in the interannual variability of the hydroclimate of central-south Chile.

2.6 Other Processes Relevant to Water Resources

The search for sustainable human development in subtropical arid climates in Chile calls for the prospection of non-conventional water resources. Present projections for climate evolution in these areas under different GHG emission scenarios

anticipate a decreasing trend in annual precipitation (e.g. Schulz et al. 2011) and inland warming, both contributing to increase aridity indices. Small coastal communities along northern Chile could benefit from cloud-water collection in areas where highly-persistent coastal low-clouds (i.e. stratocumulus clouds: Sc) are intercepted by coastal orography. A key aspect when assessing the potential of this fresh-water resource is the projection of the future evolution and seasonal variability of Sc frequency, cloud base and top heights, liquid water content and drop-size distribution (e.g. Klemm et al. 2012). Besides the necessary research on these physical climate issues, improved designs of water collecting devices are of utmost importance both in terms of efficiency and adequate structures to withstand episodic high-wind storms.

Early experiences in Chile were developed at the Universidad Católica del Norte (Antofagasta) (e.g. Lleal i Galceran 1987, and references therein). In the late 1980s, the *Camanchacas Chile* International Project was carried on at El Tofo, north of La Serena, aimed at studying the collection efficiency of low-cost rectangular meshes. Ultimately, the idea was to supply fresh-water to Chungungo, a nearby fishermen village (Schemenauer et al. 1988; Fuenzalida et al. 1989). Ongoing monitoring and research initiatives are taking place at Fray Jorge relict forest (e.g. Garreaud et al. 2008), at Alto Patache, Iquique (e.g. Muñoz-Schick et al. 2001) and Talinay (e.g. Rutllant et al. 2017). Results from these experiments have permitted the recognition of episodic strong water collection events in connection with the rear edge of coastal lows with northwesterly winds (advective *camanchacas*), and other more frequent, albeit less intense, orographic lifting events of the moist marine boundary layer air under southerly winds (orographic *camanchacas*) (e.g. Cereceda et al. 2002).

A simple calculation provides an order of magnitude of this fresh water resource. Consider a fog-collection mesh with surface area A (m^2) and a cloud with liquid water content L (l m^{-3}), moving across the mesh with speed U (m s^{-1}) perpendicular to it. Then the cloud volume crossing the mesh in 1 s is UA ($\text{m}^3 \text{s}^{-1}$), and the collected water would be αUAL ($\text{l m}^{-2} \text{s}^{-1}$), where the collecting efficiency α (typically 10%) depends on the cloud droplet size distribution, mesh material and framework. Since characteristic collected water volumes range between 2 and 12 $\text{lt m}^{-2} \text{day}^{-1}$ and assuming 8 days of water collection per month during 6 months, mean annual collected water volume would be around 250 l for a 1 m^2 mesh.

References

- Aceituno P (1988) On the functioning of the southern oscillation in the South American sector. Part I: Surface climate. *Mon Weather Rev* 116:505–524
- Aceituno P (1996) Elementos del clima en el Altiplano Sudamericano. *Revista Geofísica (IPGH)* 44:37–54
- Aceituno P, Fuenzalida H, Rosenbluth B (1993) Climate along the extratropical west coast of South America. In: Mooney HA, Fuentes ER, Kronberg BI (eds) *Earth system responses to global change: contrasts between North and South America*. Academic, New York, pp 61–72

- Álvarez MS, Vera CS, Kiladis GN, Liebmann B (2016) Influence of the Madden Julian Oscillation on precipitation and surface air temperature in South America. *Clim Dyn* 46:245–262. <https://doi.org/10.1007/s00382-015-2581-6>
- Barahona CE (2013) Precipitaciones asociadas a bajas segregadas en la zona central de Chile, entre los años 2003 y 2005. Report to obtain a professional title in Meteorology, Universidad de Valparaíso
- Barahona CE (2016) Precipitación asociada a bajas segregadas en el Hemisferio Sur. MSc thesis, Universidad de Chile
- Barrett BS, Garreaud R, Falvey M (2009) Effect of the Andes Cordillera on precipitation from a midlatitude cold front. *Mon Weather Rev* 137:3092–3109. <https://doi.org/10.1175/2009-MWR2881.1>
- Barrett BS, Carrasco JF, Testino AP (2011) Madden–Julian Oscillation (MJO) modulation of atmospheric circulation and Chilean winter precipitation. *J Clim* 25:1678–1688. <https://doi.org/10.1175/JCLI-D-11-00216.1>
- Barrett BS, Campos DA, Veloso JV, Rondanelli R (2016) Extreme temperature and precipitation events in March 2015 in central and northern Chile. *J Geophys Res Atmos* 121:4563–4580
- Boisier JP, Rondanelli R, Garreaud RD, Muñoz F (2016) Anthropogenic and natural contributions to the Southeast Pacific precipitation decline and recent megadrought in Central Chile. *Geophys Res Lett* 43:413–421. <https://doi.org/10.1002/2015-GL067265>
- Boisier JP, Alvarez-Garretón C, Cordero RR, Damiani A, Gallardo L, Garreaud RD, Lambert F, Ramallo C, Rojas M, Rondanelli R (2018) Anthropogenic drying in Central-Southern Chile evidenced by long-term observations and climate model simulations. *Elem Sci Anth* 6(1):74. <https://doi.org/10.1525/elementa.328>
- Bozkurt D, Rondanelli R, Garreaud R, Arriagada A (2016) Impact of warmer eastern tropical Pacific SST on the March 2015 Atacama floods. *Mon Weather Rev* 144:4441–4460
- Cai W, Cowan T, Thatcher M (2012) Rainfall reductions over southern hemisphere semi-arid regions: the role of subtropical dry zone expansion. *Sci Rep* 2:702. <https://doi.org/10.1038/srep00702>
- Cereceda P, Osses P, Larraín H, Farias M, Lagos M, Pinto R, Schemenauer RS (2002) Advective, orographic and radiation fog in the Tarapacá region, Chile. *Atmos Res* 64:261–271
- Collins M, Knutti R, Arblaster J, Dufresne JL, Fichefet F, Friedlingstein P, Gao X, Gutowski WJ, Johns T, Krinner G, Shongwe M, Tebaldi C, Weaver AJ, Wehner M (2013) Long-term climate change: projections, commitments and irreversibility. In: Stocker TF, Qin D, Plattner GK, Tignor M, Allen SK, Boschung J, Nauels A, Xia Y, Bex V, Midgley PM (eds) *Climate change 2013: the physical science basis. Contribution of working group I to the fifth assessment report of the intergovernmental panel on climate change*. Cambridge University Press, Cambridge/New York, pp 1029–1136
- Cortés G, Vargas X, McPhee J (2011) Climatic sensitivity of streamflow timing in the extratropical western Andes Cordillera. *J Hydrol* 405:93–109
- Dee DP et al (2011) The ERA-interim reanalysis: configuration and performance of the data assimilation system. *Q J R Meteorol Soc* 137(656):553–597. <https://doi.org/10.1002/qj.828>
- Donald A, Meinke H, Power B, Maia ADHN, Wheeler MC, White N, Stone RC, Ribbe J (2006) Near-global impact of the Madden-Julian Oscillation on rainfall. *Geophys Res Lett* 33(9). <https://doi.org/10.1029/2005GL025155>
- Dong B, Dai A (2015) The influence of the Interdecadal Pacific Oscillation on temperature and precipitation over the globe. *Clim Dyn* 45:2667–2681. <https://doi.org/10.1007/s00382-015-2500-x>
- Falvey M, Garreaud R (2007) Wintertime precipitation episodes in Central Chile: associated meteorological conditions and orographic influences. *J Hydrometeorol* 8:171–193
- Fuentes R (2014) Sensibilidad a diferentes condiciones iniciales en simulaciones de mesoescala de una baja segregada: un caso de estudio. Report to obtain a professional title in Meteorology, Universidad de Valparaíso
- Fuenzalida H (1971) *Climatología de Chile*. Sección Meteorología, Departamento de Geofísica y Geodesia. Universidad de Chile, 73pp

- Fuenzalida H, Rutllant J, Vergara J (1989) Meteorological aspects of water collection from strato-cumuli in Northern Chile. Extended Abstracts 3rd international conference on southern hemisphere meteorology and oceanography, Buenos Aires, Nov 1989
- Fuenzalida H, Sánchez R, Garreaud R (2005) A climatology of cut off lows in the southern hemisphere. *J Geophys Res* 110:D1801. <https://doi.org/10.1029/2005JD005934>
- Garreaud RD (1999) A multi-scale analysis of the summertime precipitation over the Central Andes. *Mon Weather Rev* 127:901–921
- Garreaud R (2007) Precipitation and circulation covariability in the extratropics. *J Clim* 20:4789–4797
- Garreaud R (2013) Warm winter storms in Central Chile. *J Hydrometeorol* 14:1515–1534. <https://doi.org/10.1175/JHM-D-12-0135.1>
- Garreaud RD, Aceituno P (2001) Interannual rainfall variability over the South American Altiplano. *J Clim* 14:2779–2789
- Garreaud R, Battisti DS (1999) Interannual (ENSO) and Interdecadal (ENSO-like) variability in the southern hemisphere tropospheric circulation. *J Clim* 12:2113–2123
- Garreaud R, Fuenzalida HA (2007) The influence of the Andes on cut-off lows: a modeling study. *Mon Weather Rev* 135:1596–1613
- Garreaud R, Rutllant J (1996) Análisis meteorológico de los aluviones de Antofagasta y Santiago de Chile en el periodo 1991–1993. *Atmósfera* 9:251–271
- Garreaud R, Vuille M, Clements A (2003) The climate of the Altiplano: observed current conditions and past change mechanisms. *Paleo* 3054:1–18
- Garreaud R, Barichivich J, Christie DA, Maldonado A (2008) Interannual variability of the coastal fog at Fray Jorge relict forests in semiarid Chile. *J Geophys Res* 113. <https://doi.org/10.1029/2008JG000709>
- Garreaud R, Lopez P, Minvielle M, Rojas M (2013) Large scale control on the Patagonia climate. *J Clim* 26:215–230
- Garreaud R, Falvey M, Montecinos A (2016) Orographic precipitation in coastal southern Chile: mean distribution, temporal variability and linear contribution. *J Hydrometeorol* 17:1185–1202
- Garreaud RD, Alvarez-Garretón C, Barichivich J, Boisier JP, Christie D, Galleguillos M, LeQuesne C, McPhee J, Zambrano-Bigiarini M (2017) The 2010–2015 megadrought in Central Chile: impacts on regional hydroclimate and vegetation. *Hydrol Earth Syst Sci* 21:6307–6327. <https://doi.org/10.5194/hess-21-6307-2017>
- Garreaud R, Boisier JP, Rondanelli R, Montecinos A, Sepúlveda H, Veloso-Águila D (2019) The Central Chile mega drought (2010–2018): a climate dynamics perspective. *Int J Climatol* 40(1):421–439. <https://doi.org/10.1002/joc.6219>
- Gillett NP, Kell TD, Jones PD (2006) Regional climate impacts of the southern annular mode. *Geophys Res Lett* 33. <https://doi.org/10.1029/2006GL027721>
- Gillett NP, Fyfe JC, Parker DE (2013) Attribution of observed sea level pressure trends to greenhouse gas, aerosol, and ozone changes. *Geophys Res Lett* 40:2302–2306. <https://doi.org/10.1002/grl.50500>
- Grimm AM, Barros VR, Doyle ME (2000) Climate variability in southern South America associated with El Niño and La Niña events. *J Clim* 13:35–58. [https://doi.org/10.1175/1520-0442\(2000\)013<0035:CVISSA>2.0.CO;2](https://doi.org/10.1175/1520-0442(2000)013<0035:CVISSA>2.0.CO;2)
- Guan B, Waliser DE (2015) Detection of atmospheric rivers: evaluation and application of an algorithm for global studies. *J Geophys Res Atmos* 120:12514–12535. <https://doi.org/10.1002/2015JD024257>
- Haylock MR, Peterson TC, Alves LM, Ambrizzi T, Anunciação YMT, Baez J, Barros VR, Berlatto MA, Bidegain M, Coronel G, Corradi V, Garcia VJ, Grimm AM, Karoly D, Marengo JA, Marino MB, Moncunill DF, Nechet D, Quintana J, Rebello E, Rusticucci M, Santos JL, Trebejo I, Vincent LA (2006) Trends in total and extreme south American rainfall in 1960–2000 and links with sea surface temperature. *J Clim* 19:1490–1512. <https://doi.org/10.1175/JCLI3695.1>
- Houston J, Hartley AJ (2003) The central Andean west-slope rainshadow and its potential contribution to the origin of hyper-aridity in the Atacama Desert. *Int J Climatol* 23:1453–1464

- Jacques-Coper M, Garreaud RD (2015) Characterization of the 1970s climate shift in South America. *Int J Climatol* 35:2164–2179. <https://doi.org/10.1002/joc.4120>
- Jiménez-Cisneros BE, Oki T, Arnell NW, Benito G, Cogley JG, Döll P, Jiang T, Mwakalila SS (2014) Freshwater resources. In: Field CB, Barros VT, Dokken DJ, Mach KJ, Mastrandrea MD, Bilir TE, Chatterjee M, Ebi KL, Estrada YO, Genova RC, Girma B, Kissel ES, Levy AN, MacCracken S, Mastrandrea OR, White LL (eds) *Climate change 2014: impacts, adaptation, and vulnerability. Part A: global and sectoral aspects. Contribution of working group II to the fifth assessment report of the intergovernmental panel of climate change*. Cambridge University Press, Cambridge/New York, pp 229–269
- Juliá C, Rahn DA, Ruttant JA (2012) Assessing the influence of the MJO on strong precipitation events in subtropical, semi-arid North-Central Chile (30°S). *J Clim* 25:7003–7013
- Karoly DJ (1989) Southern hemisphere circulation features associated with el Niño-southern oscillation events. *J Clim* 2:1239–1252. [https://doi.org/10.1175/1520-0442\(1989\)002<1239:SHCFAW>2.0.CO;2](https://doi.org/10.1175/1520-0442(1989)002<1239:SHCFAW>2.0.CO;2)
- Klemm O, Schemenauer RS, Lummerich A, Cereceda P, Marzol V, Corell D, van Heerden J, Reinhard D, Gherezghiher T, Olivier J, Osses P, Sarsour J, Frost E, Estrela M, Valiente JA, Mussie Fessehaye G (2012) Fog as a fresh-water resource: overview and perspectives. *Ambio* 41(3):221–234. <https://doi.org/10.1007/s13280-012-0247-8>
- Lenters JD, Cook KH (1997) On the origin of the Bolivian high and related circulation features of the South American climate. *J Atmos Sci* 54:656–677
- Lleal i Galceran F (1987) La Camanchaca: Captacions d'aigua al Desert d'Atacama. *Revista Catalana de Geografia* 5(II):59–69
- Marqués R, Rao VB (1999) A diagnosis of a long-lasting blocking event over the Southeast Pacific Ocean. *Mon Weather Rev* 127:1761–1776
- Marshall GJ (2003) Trends in the southern annular mode from observations and reanalyses. *J Clim* 16(24):4134–4143. [https://doi.org/10.1175/1520-0442\(2003\)016<4134:TITSAM>2.0.CO;2](https://doi.org/10.1175/1520-0442(2003)016<4134:TITSAM>2.0.CO;2)
- Minetti JL, Vargas WM, Poblete AG, Acuña LR, Grande GC (2003) Non-linear trends and low frequency oscillations in annual precipitation over Argentina and Chile, 1931–1999. *Atmósfera* 16:119–135
- Mo KC, Higgins RW (1998) The Pacific–South American modes and tropical convection during the southern hemisphere winter. *Mon Weather Rev* 126:1581–1596. [https://doi.org/10.1175/1520-0493\(1998\)126<1581:TPSAMA>2.0.CO;2](https://doi.org/10.1175/1520-0493(1998)126<1581:TPSAMA>2.0.CO;2)
- Mo KC, Paegle JN (2001) The Pacific–south American modes and their downstream effects. *Int J Climatol* 21:1211–1229. <https://doi.org/10.1002/joc.685>
- Montecinos A, Aceituno P (2003) Seasonality of the ENSO-related rainfall variability in Central Chile and associated circulation anomalies. *J Clim* 16:281–296. [https://doi.org/10.1175/1520-0442\(2003\)016<0281:SOTERR>2.0.CO;2](https://doi.org/10.1175/1520-0442(2003)016<0281:SOTERR>2.0.CO;2)
- Muñoz-Schick M, Pinto R, Mesa A, Moreira-Muñoz A (2001) Oasis de neblina en los cerros costeros del sur de Iquique, región de Tarapacá, Chile, durante el evento El Niño 1997–1998. *Rev Chil Hist Nat* 74:389–405
- Ndarana T, Waugh DW (2010) The link between cut-off lows and Rossby wave breaking in the southern hemisphere. *Q J R Meteorol Soc* 136:869–885
- O’Kane TJ, Monselesan DP, Risbey JS (2016) A multiscale reexamination of the Pacific–south American pattern. *Mon Weather Rev* 145:379–402. <https://doi.org/10.1175/MWR-D-16-0291.1>
- Palmen E (1949) On the origin and structure of high level cyclones south of the maximum westerlies. *Tellus* 1:22–31
- Pizarro JG, Montecinos A (2000) Cut-off cyclones off the subtropical coast of Chile. Preprints 6th international conference on southern hemisphere meteorology and oceanography. American Meteorological Society, pp 278–279
- Polade SD, Gershunov A, Cayan DR, Dettinger MD, Pierce DW (2017) Precipitation in a warming world: assessing projected hydro-climate changes in California and other Mediterranean climate regions. *Sci Rep* 7(1):10783. <https://doi.org/10.1038/s41598-017-11285-y>

- Purich A, Cowan T, Min S-K, Cai W (2013) Autumn precipitation trends over southern hemisphere midlatitudes as simulated by CMIP5 models. *J Clim* 26:8341–8356. <https://doi.org/10.1175/JCLI-D-13-00007.1>
- Quintana JM, Aceituno P (2012) Changes in the rainfall regime along the extratropical west coast of South America (Chile): 30–43° S. *Atmósfera* 25:1–22
- Ralph FM, Dettinger M, Lavers D, Gorodetskaya IV, Martin A, Viale M, White AB, Oakley N, Rutz J, Spackman JR, Wemli H, Cordeira J (2017) Atmospheric rivers emerge as a global science and applications focus. *Bull Am Meteor Soc* 98:1969–1973. <https://doi.org/10.1175/BAMS-D-16-0262.1>
- Rao VB, do Carmo AMC, Franchito SH (2003) Interannual variations of storm tracks in the southern hemisphere and their connections with the Antarctic oscillation. *Int J Climatol* 23:1537–1545. <https://doi.org/10.1002/joc.948>
- Renwick JA, Revell MJ (1999) Blocking over the South Pacific and Rossby wave propagation. *Mon Weather Rev* 127:2233–2247. [https://doi.org/10.1175/15200493\(1999\)127<2233:BOTS PA>2.0.CO;2](https://doi.org/10.1175/15200493(1999)127<2233:BOTS PA>2.0.CO;2)
- Renwick JA (2005) Persistent positive anomalies in the Southern Hemisphere circulation. *Mon Weather Rev* 133:977–988
- Rondanelli R, Hatchett B, Rutllant J, Bozkurt D, Garreaud R (2019) Strongest MJO on record triggers extreme Atacama rainfall and warmth in Antarctica. *Geophys Res Lett* 46. <https://doi.org/10.1029/2018GL081475>
- Rutllant J, Fuenzalida H (1991) Synoptic aspects of the Central Chile rainfall variability associated with the Southern Oscillation. *Int J Climatol* 11:63–76. <https://doi.org/10.1002/joc.3370110105>
- Rutllant JA, Reyes A, Rondanelli R, Mardones P (2017) Campaña Talinay 2016: Coherencia especial de las observaciones intensivas realizadas entre el 18 y 28 de Octubre. V Congreso de Oceanografía Física, Meteorología y Clima del Pacífico Sur-Oriental. 6–10 Noviembre 2017, U. de Concepción
- Scaff L, Rutllant JA, Rahn D, Gascoïn S, Rondanelli R (2017) Meteorological interpretation of orographic precipitation gradients along an Andes West slope basin at 30° S (Elqui Valley, Chile). *J Hydrometeorol* 18:713–727
- Schemenauer R, Fuenzalida H, Cereceda P (1988) A neglected water resource: the *Camanchaca* of South America. *Bull Am Meteorol Soc* 69:138–147
- Schewe J, Heinke J, Gerten D, Haddeland I, Arnell NW, Clark DB, Dankers R, Eisner S, Fekete BM, Colón-González FJ, Gosling SN, Kim H, Liu X, Masaki Y, Portmann FT, Satoh Y, Stacke T, Tang Q, Wada Y, Wisser D, Albrecht T, Frieler K, Piontek F, Warszawski L, Kabat P (2014) Multimodel assessment of water scarcity under climate change. *PNAS* 111:3245–3250. <https://doi.org/10.1073/pnas.1222460110>
- Schulz N, Boisier JP, Aceituno P (2011) Climate change along the arid coast of northern Chile. *Int J Climatol* 32:1803–1814. <https://doi.org/10.1002/joc.2395>
- Sinclair MR, Renwick JA, Kidson JW (1997) Low-frequency variability of southern hemisphere sea level pressure and weather system activity. *Mon Weather Rev* 125:2531–2543. [https://doi.org/10.1175/1520-0493\(1997\)125<2531:LFOVSH>2.0.CO;2](https://doi.org/10.1175/1520-0493(1997)125<2531:LFOVSH>2.0.CO;2)
- Smith RB, Evans JP (2007) Orographic precipitation and water vapor fractionation over the southern Andes. *J Hydrometeorol* 8:3–19
- Taylor KE, Stouffer RJ, Meehl GA (2011) An overview of CMIP5 and the experiment design. *Bull Am Meteorol Soc* 93(4):485–498. <https://doi.org/10.1175/BAMS-D-11-00094.1>
- Thompson DWJ, Wallace JM (2000) Annular modes in the extratropical circulation. Part I: month-to-month variability. *J Clim* 13:1000–1016. [https://doi.org/10.1175/1520-0442\(2000\)013<1000:AMITEC>2.0.CO;2](https://doi.org/10.1175/1520-0442(2000)013<1000:AMITEC>2.0.CO;2)
- Vera C, Higgins W, Amador J, Ambrizzi T, Garreaud R, Gochis D, Gutzler D, Lettenmaier D, Marengo J, Mechoso C, Noguez-Paele J, Silva Diaz PL, Zhang C (2006) Towards a unified view of the American monsoon system. *J Clim* 19:4977–5000
- Viale M (2017) Technical note. <http://www.dgf.uchile.cl/noticias/140021/aluvion-en-villa-santa-lucia-y-su-relacion-con-un-rio-atmosferico>

- Viale M, Garreaud R (2014) Summer precipitation events over the western slope of the subtropical Andes. *Monthly Weather Review* 142:1074–1092
- Viale M, Garreaud R (2015) Orographic effects of the subtropical and extratropical Andes on upwind precipitating clouds. *J Geophys Res Atmos* 120. <https://doi.org/10.1002/2014JD023014>
- Viale M, Núñez MN (2011) Climatology of winter orographic precipitation over the subtropical Central Andes and associated synoptic and regional characteristics. *J Hydrometeorol* 12:481–507
- Viale M, Valenzuela R, Garreaud RD, Ralph FM (2018) Impacts of atmospheric rivers on precipitation in Southern South America. *J Hydrometeorol* 19:1671–1687. <https://doi.org/10.1175/JHM-D-18-0006.1>